

Formation control of multiple vehicles using dynamic surface control and hybrid systems

ANOUCK R. GIRARD^{†*} and J. KARL HEDRICK[†]

This paper deals with the formation control of multiple vehicles, using a combination of dynamic surface sliding control and hybrid systems. Each vehicle must perform several manoeuvres, either independently, or in a coordinated fashion as part of a vehicle formation. A dynamic surface controller is designed for each manoeuvre. Switches between manoeuvres and communication protocols between vehicles are represented using hybrid systems formalisms. Here, we present the design of both independent and coordinated dynamic positioning (DP) controllers for ocean vehicles using dynamic surface control. Independent and coordinated dynamic positioning are manoeuvres that the modules forming a floating runway at sea must perform. Experimental results using scaled modules are shown.

1. Introduction

There are many applications where ‘coordinated’ control of multiple vehicles or systems is desirable. For instance, in the automotive field, various stages of automation lead to applications ranging from automated highway systems to coordinated adaptive cruise control systems, to ‘platooning’ of passenger and military vehicles.

Also, there is a trend in the military towards autonomous air, ground and ocean vehicles; these vehicles perform coordinated missions and require some communicated information among them. Some of these applications include coordinated ocean platform control for the mobile offshore base (MOB), coordinated operation of several autonomous underwater vehicles (AUVs), and/or of unmanned combat air vehicles (UCAVs). Each of these applications requires communications between multiple autonomous vehicles, so as to achieve cooperation, and in that sense the vehicles are networked. Wireless communications are used frequently, as they are well suited to autonomous vehicle problems.

We will use the control of ocean vehicles as an example throughout this paper. In particular, we will consider the MOB, a very large floating ocean structure meant to provide capabilities similar to that of an on-land army base. It must accommodate the landing and take-off of C-17 conventional aircraft, host 3000 troops, carry 10 million gallons of fuel and provide 3 million square feet of internal re-configurable storage. A MOB is formed of several modules, which must perform long-term station keeping at sea in the presence of wind, waves and currents. This is usually referred to as dynamic positioning (DP). The relative alignment

between modules has to be kept tight so planes can land on the runway, while the assembly as a whole is allowed to drift within reason. Dynamic positioning of several ocean structures with respect to each other is a difficult problem, and despite a wealth of possible applications and spin-offs (thruster-assisted mooring, cargo transfer, at-sea refueling, etc.), is not commonplace in the industry.

Here we present a dynamic surface controller for stand-alone and coordinated dynamic positioning control of ocean vehicles/structures. The controller is shown to be stable, and tracking errors to be bounded. The use of a modern control methodology like dynamic surface control (DSC) has several advantages over PID controllers, which are still the industry standard. Multiple-input, multiple-output PID controllers require extensive tuning. DSC takes uncertainties directly into account in the controller design, and offers stability and robustness guarantees. For a detailed description of DSC, the reader is referred to Swaroop *et al.* (1997, 2001). One of the attributes of DSC is to select the controlled variable to make the time derivative of a Lyapunov function candidate negative definite. The proposed modification of DSC draws on a choice of a particular Lyapunov function candidate proposed by Slotine and Li (1991) for the control of a class of robotic systems. Other similar methods include integrator backstepping (IB) (Krstic *et al.* 1995) and multiple sliding surface control (MSSC) (Won and Hedrick 1996). To overcome some shortcomings of IB and MSSC (such as model differentiation and explosion of terms), DSC avoids model differentiation by using a bank of first-order filters. If the non-linearities in the system are Lipschitz, the DSC algorithm guarantees global exponential regulation and arbitrarily bounded tracking. If the non-linearities are non-Lipschitz, semi-global arbitrarily bounded regulation and tracking are guaranteed (Girard and Hedrick 2001, Swaroop *et al.* 2001).

Operating a multi-module runway such as the MOB at sea implies not only station-keeping capabilities, but

Received 15 May 2002. Revised 23 September 2002.
Accepted 30 November 2002.

* Author for correspondence. e-mail: anouck@eecs.berkeley.edu

† The University of California at Berkeley, Berkeley, CA 94720, USA. e-mail: khedrick@me.berkeley.edu

also the ability to bring modules together to form the runway, the ability to separate modules from the runway, and the ability to perform coordinated manoeuvres, such as rotating the assembly into the wind. The necessity to have several different manoeuvres for the MOB raises questions as to how to transition gracefully from one manoeuvre into the next. Several approaches to mode switching for multi-vehicle systems are described in the literature. Our observation is that they generally do not deal with the problem of transitioning smoothly from one mode into the next, which is an issue for passenger comfort and hardware longevity. Moreover, existing approaches do not usually account for scalability.

This paper is organized as follows: in a first time, we will apply this modified DSC approach to the problem of dynamic positioning for stand-alone and multiple semi-submersible platforms forming a MOB; we present the equations of motion and the dynamic surface controller design for the dynamic positioning of MOB modules. The concepts developed in this project have been validated by physical experiments with scaled MOB modules. A brief overview of the hardware is given, along with experimental results for both independent and coordinated DP. We also present an example communication protocol for the docking scenario for a MOB and show some experimental results.

2. Dynamic surface controller design for the dynamic positioning of ships and offshore platforms

The equations of motion of a platform when derived in their complete form are quite complex, not only because of the sheer number of equations and forces, but also because the hydrodynamic force models are complex. In this section, we present the low frequency model of the platform dynamics that was implemented and used for the controller design. This model describes the motions of the dynamically positioned system.

The motion of the body-fixed frame is described relative to an inertial frame. The inertial frame is denoted (X_E, Y_E, Z_E) where the subscript ‘E’ stands for ‘Earth-fixed’. Typically the inertial frame is chosen so that X_E points north, Y_E points east, and Z_E points downward towards the centre of the Earth. Consider for now the 2D problem. In the (X_E, Y_E, Z_E) frame, the platform has a position vector η , with components $[x, y, \psi]$, where x and y designate the position and ψ is the heading angle. In the inertial frame a velocity vector, $\dot{\eta}$ can also be defined, with components $[\dot{x}, \dot{y}, \dot{\psi}]$.

The position and the velocity are vectors, and can be expressed in any basis. It is convenient when thinking about vehicles to define a body-fixed frame, say (X, Y, Z) . The Society of Naval Architects and Marine Engineers (SNAME) has dictated standards for choos-

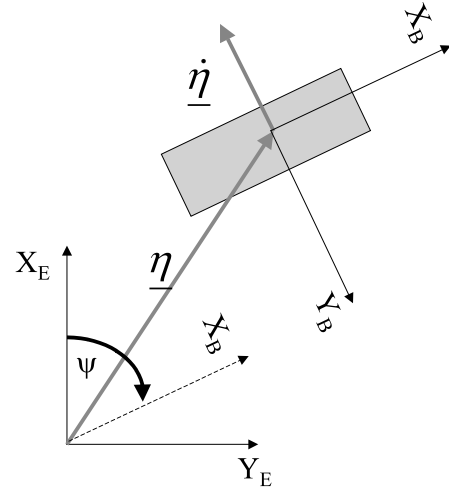


Figure 1. Inertial (Earth-fixed) and body-fixed frames for the derivation of the equations of motion.

ing the body-frame (Fossen 1994), so that the X -position is directed from aft to fore, the Y -position is directed to starboard, and Z is pointing downward, as shown in figure 1.

A free-floating body in the ocean moves in all six degrees of freedom. In dynamic positioning of vessels, we want to control a vessel (or platform) on the ocean surface with respect to the ocean floor. This is because traditionally, dynamic positioning is used to connect an oil well on the sea floor with a vessel on the surface using a pipeline. Dynamic positioning vessels are not generally equipped with actuators in heave, roll or pitch. We consider the two-dimensional problem where we deal with the surge (X_B -position), sway (Y_B -position) and yaw (rotation about Z_B) motions.

The equations of motion which describe the low-frequency motion of a surface vessel can be written in the body-fixed frame as (Newman 1977)

$$M\dot{\nu} + C(\nu)\nu + D(\nu)\nu = \tau + \tau_{\text{env}} \quad (1)$$

$$\dot{\eta} = J(\eta)\nu \quad (2)$$

where:

- $\nu = [u \ v \ r]^T$ is formed of the body-fixed components of the Earth-fixed velocity vector of the platform,
- $\dot{\eta} = [\dot{x} \ \dot{y} \ \dot{\psi}]^T$ is the velocity of the platform in the inertial frame,
- M is the mass plus added mass matrix of the platform (from the physical standpoint, the added mass represents the amount of fluid accelerated with the body),
- $C(\nu)$ is the Coriolis and centripetal matrix,
- $D(\nu)$ is the damping matrix,

- τ represents the body-fixed forces from the actuators,
- τ_{env} represents viscous drag and forces due to the environment (wind, waves and currents), and
- $J(\eta)$ is a transformation matrix between the inertial and body-fixed coordinate frames, with:

$$J(\eta) = \begin{bmatrix} \cos(\psi) & -\sin(\psi) & 0 \\ \sin(\psi) & \cos(\psi) & 0 \\ 0 & 0 & 1 \end{bmatrix} \quad (3)$$

In these equations we have assumed zero current velocity as a simplification for controller design. Also, the equations are in two dimensions (that is, we consider three degrees of freedom). The thrusters only counteract the ‘horizontal’ forces and act in surge, sway and yaw. The ‘vertical’ motions, heave (Z_B position), roll (rotation about X_B) and pitch (rotation about Y_B), are not considered here. For conventional ships and platforms, rolling and pitching motions have zero-mean and limited amplitude.

The total motion of the ship in waves is given by the sum of a low-frequency component and a wave-frequency motion. The low-frequency component is separated out from the measured total ship motions by a wave filtering system. Attempting to control the oscillatory motion due to the waves causes wear and tear on the thrusters, and in general actuator bandwidth is insufficient to counter those motions efficiently. Several filters as well as a non-linear observer have been developed for the filtering of these motions (Girard 1999).

2.1. Non-linear control of one vessel

The control problem is to choose the actuator forces to be applied such that the vessel reaches desired inertial coordinates

$$\eta_d = [x_d, y_d, \Psi_d]^T \quad (4)$$

We utilize the multiple sliding surface (MSS) (Won and Hedrick 1996) and dynamic surface control (DSC) (Swaroop *et al.* 1997) methods as well as the ‘Slotine and Li’ algorithm (Slotine and Li 1991), which was adapted to the control of underwater vehicles by Fossen (1994).

The MSS controller involves two ‘sliding surfaces’ (Utkin 1992, 1977, Utkin *et al.* 1999). The first surface defines the desired vessel position and orientation. The second surface defines a desired velocity, which, if maintained, will drive the vessel to its desired position. Thruster forces are chosen such that the second surface approaches zero.

The first surface is defined as

$$s_1 = \eta - \eta_d \quad (5)$$

Differentiating s_1 yields

$$\dot{s}_1 = J(\eta)\nu - \dot{\eta}_d \quad (6)$$

At this point a desired velocity, or ‘synthetic control’, ν_d is defined as

$$J(\eta)\nu_d = \dot{\eta}_d - A_1 s_1 \quad (7)$$

where A_1 is a positive definite matrix. With this definition, if $\nu = \nu_d$, then

$$\dot{s}_1 = -A_1 s_1 \quad (8)$$

and $s_1 \rightarrow 0$ with a convergence rate determined by the choice of A_1 . Because of the definition of s_1 , this will also guarantee that $\eta \rightarrow \eta_d$.

The second sliding surface could be defined as $s_2 = \nu - \nu_d$, but computing the derivative of s_2 could lead to a very complex control law. A method called dynamic surface control (DSC) and described by Swaroop *et al.* (1997) eliminates the need for model differentiation. First, we pass ν_d through a bank of first order filters

$$T\dot{z} + z = \nu_d \quad (9)$$

where T is a diagonal matrix whose elements, T_{ii} , are the filter time constants. These are chosen to be as small as possible, consistent with numerical conditioning problems. ‘ z ’ now serves as an estimate of ν_d , with a derivative that is easily computed as

$$\dot{z} = T^{-1}(\nu_d - z) \quad (10)$$

Using z in place of ν_d , we now define the second sliding surface as

$$s_2 = \nu - z \quad (11)$$

At this point, a Lyapunov approach (Slotine and Li 1991) can be drawn upon. We select a Lyapunov function candidate to be

$$V = \frac{1}{2} s_2^T M s_2 \quad (12)$$

Differentiating V and using equations (1) and (11) yields

$$\dot{V} = s_2^T [M\dot{\nu} - M\dot{z}] = s_2^T [\tau_T - C(\nu)\nu - M\dot{z}] \quad (13)$$

where τ_T , the thruster force, is considered the only force acting on the vessel for the purpose of controller design. If τ_T is selected as

$$\tau_T = C(\nu)\nu + M\dot{z} - K_D s_2 \quad (14)$$

where K_D is a positive definite, symmetric gain matrix, then

$$\dot{V} = -s_2^T K_D s_2 \quad (15)$$

which guarantees that $s_2 \rightarrow 0$. This in turn implies that $\nu \rightarrow \nu_d$, $s_1 \rightarrow 0$ and $\eta \rightarrow \eta_d$. Using equation (10), the control law can be written in terms of z

$$\tau_T = C(\nu)\nu + MT^{-1}(\nu_d - z) - K_D s_2 \quad (16)$$

2.2. Control of multiple vessels

There are a great number of different possible strategies for coordinating MOBs. The goal of every strategy is to position the vessels in a straight line with tight relative spacing constraints. Three control strategies have been tested and implemented (Hedrick *et al.* 1999), using either the first or the middle modules as leaders in follow-the-leader type algorithms or using leaderless control where each module tracks an inertial reference and maintains a desired relative spacing with respect to the other modules. The best results were produced by this last approach, using:

$$\text{1st vessel: } s_1^1 = \eta^1 - \eta_d^1 + A_r(\eta^1 - \eta^2 - \eta_d^2) \quad (17)$$

$$\begin{aligned} \text{2nd vessel: } s_1^2 = & \eta^2 - \eta_d^2 + A_r(\eta^2 - \eta^1 - \eta_d^1) \\ & + A_r(\eta^2 - \eta^3 - \eta_d^3) \end{aligned} \quad (18)$$

$$\text{3rd vessel: } s_1^3 = \eta^3 - \eta_d^3 + A_r(\eta^3 - \eta^2 - \eta_d^2) \quad (19)$$

where η_d^{ij} is the desired relative spacing between modules i and j . The above notation allows us to see clearly the interactions of the two separate terms, with the first part of each s_1 surface dealing with tracking an inertial position and the second part dealing with adjustments to the relative position. One reason to separate both terms so explicitly is that for the MOB, the absolute position of the assembled platforms does not have tight requirements, as pilots can easily spot the structure from the air or receive broadcasts giving the exact position of the floating runway. However, fuel economy is a significant issue, and the assembled MOB should be allowed to drift within reason. Yet the relative alignment of the platforms is of paramount importance for landing planes. The two-tiered control laws as presented in equations (17)–(19) allow us to make this distinction clear. If one only uses absolute positions, fuel consumption may be higher than needed. If one only controls relative platform positions, the assembly may drift significantly.

By adjusting the diagonal elements of A_r , the importance of absolute vs. relative errors can be changed, with higher values corresponding to tighter relative position accuracy. Some of the attractive features of this approach are: (1) there is guaranteed string stability (Swaroop and Hedrick 1996) since each vessel has an inertial reference, and (2) the identical control structure can be used for both de-coupled and coupled manoeuvres. If it is desired to de-couple the vessels and send them to arbitrary locations, then $A_r \equiv 0$ and η_d^i is defined for each separate vessel. Here by coupled we mean that the modules directly consider the position

of their neighbours (coordinated positioning), and by decoupled we mean that the modules act independently of one another.

2.3. Adaptive approach

When the model parameters are not perfectly known, the controller must be implemented using estimated parameters. In this case, equation (16) becomes

$$\tau_T = \hat{C}(\nu)\nu + \hat{M}\dot{z} - K_D s_2 \quad (20)$$

where the superscript ‘‘ $\hat{\cdot}$ ’’ designates estimated values. With the gain matrix K_D chosen large enough, this control can keep s_2 arbitrarily close to zero even in the presence of large modelling errors. Therefore, this is a robust controller.

For a number of reasons, achieving robustness through the use of high-gains is often undesirable. An alternative approach for dealing with parameter uncertainty is to use an adaptation algorithm, such as the one outlined in Swaroop *et al.* (2001). If the unknown parameters are constants that appear linearly in the system of equations, then equation (20) can be written in the form

$$\tau_T = Y(\nu, \dot{z})\hat{a} - K_D s_2 \quad (21)$$

where \hat{a} is a p^*1 vector of estimated model parameters (we adapt on p different model parameters) and Y is an exactly known 3^*p matrix. For the true a

$$C(\nu)\nu + M\dot{z} = Y(\nu, \dot{z})a \quad (22)$$

A candidate Lyapunov function is chosen to be

$$V = \frac{1}{2}s_2^T M s_2 + \frac{1}{2}\tilde{a}^T \Gamma^{-1} \tilde{a} \quad (23)$$

where $\tilde{a} = \hat{a}(t) - a$, a is the vector of unknown constants and Γ is a symmetric positive definite matrix. By differentiating and substituting, \dot{V} is found to be

$$\dot{V} = -s_2^T K_D s_2 + (s_2^T Y + \tilde{a}^T \Gamma^{-1})\tilde{a} \quad (24)$$

If the parameter adaptation law is defined as

$$\dot{\hat{a}} = -\Gamma Y^T s_2 \quad (25)$$

then

$$\dot{V} = -s_2^T K_D s_2 \quad (26)$$

This guarantees that $s_2 \rightarrow 0$, even in the presence of model error. The complete adaptive control law to be implemented consists of equations (5), (10), (11), (14), (21) and (25).

3. Stability analysis—bounded tracking error

The idea of a stable system is familiar to most of us. Intuitively, a stable system is one that, when perturbed from an equilibrium state, will tend to return to that state (Khalil 2001). When one considers non-linear

systems, he/she encounters complicated, and at times exotic, behaviour. For a detailed description of stability considerations for non-linear systems, the reader is referred to Slotine and Li (1991) and Khalil (2001). In this section we will consider a slightly more general form of systems than have been considered in the previous section. By design, dynamic surface controllers are stable, as the control law is selected to make a Lyapunov function candidate negative definite. Here we examine considerations relating to the boundedness of the tracking error for our particular class of systems.

We consider systems of the form

$$M(\eta)\ddot{\eta} + C(\eta, \dot{\eta})\dot{\eta} + D(\eta, \dot{\eta})\dot{\eta} + g(\eta) = \tau + \tau_{\text{act}} \quad (27)$$

where:

- η is the position of the system,
- M is the mass (+ added mass, for ships) matrix of the system, M is symmetric positive definite,
- C is the Coriolis and centripetal matrix,
- D is the damping matrix,
- $g(\eta)$ represents gravitational effects,
- τ_{act} represents the forces from the actuators, and
- τ represents un-modeled external forces and moments.

The (feedback) control problem for systems in this class is to compute the desired actuator inputs to achieve desired system tasks (such as station keeping, trajectory tracking etc.). The ship dynamic positioning control problem as stated previously falls into this category. A number of robotics applications also belong to this class of systems. In ship control problems, the standard environment is the ocean, which is very variable, and difficult to bound.

3.1. Transformation to standard form

In general the first step for the DSC method is to feedback-linearize the system. The controller is then designed on the transformed system. The derivation of a feedback linearizing transformation for our class of systems is straightforward. Taking τ_{act} to be of the form:

$$\tau_{\text{act}} = M(\eta)v_{\text{syn}} + C(\eta, \dot{\eta})\dot{\eta} + D(\eta, \dot{\eta})\dot{\eta} + g(\eta) \quad (28)$$

where v_{syn} is the new control input yields

$$\ddot{\eta} = v_{\text{syn}} \quad (29)$$

Define the tracking error as

$$\tilde{\eta} = \eta - \eta_d \quad (30)$$

Then letting

$$v = \ddot{\eta}_d - 2\lambda\dot{\tilde{\eta}} - \lambda^2\tilde{\eta} \quad (\lambda > 0) \quad (31)$$

leads to exponentially stable closed-loop dynamics

$$\ddot{\tilde{\eta}}_d - 2\lambda\dot{\tilde{\eta}} - \lambda^2\tilde{\eta} = 0 \quad (32)$$

in the absence of input saturation.

The above development assumes that the dynamic model is perfect and the disturbances are zero. At this point one usually examines the disturbances to get information such as bounds, Lipschitz properties etc. Unfortunately, experts disagree on how to bound environmental forces and loads on ocean structures, and on whether or not this is possible in general. We therefore consider the general case of non-Lipschitz disturbances.

3.2. DSC design for systems with non-Lipschitz nonlinearities

3.2.1. *Form of system.* Let us write the system in the form

$$x_1 = \eta, x_2 = \dot{\eta} \quad (33)$$

$$\dot{x}_1 = x_2 + \Delta f_1(x_1) \quad (34)$$

$$\dot{x}_2 = v_{\text{syn}} + f_2(x_1, x_2) + \Delta f_2(x_1, x_2) \quad (35)$$

In this form, the expressions for the derivatives are basically the sum of a linear system in controllable form, plus a known non-linearity (the function f_2), plus an unknown non-linearity in each channel (the Δf_i). With this notation, the objective of the controller is to make x_1 track x_{1d} .

3.2.2. *Assumptions.* We assume that:

- (a) $|\Delta f_i(x_1, x_2)| \leq \rho_i(x_1, x_2)$, $i = 1, 2$ where the ρ_1 is a C^1 function in x_1 and ρ_2 is a C^1 function in x_1, x_2 . The ρ_i are not required to be globally Lipschitz in their arguments, and the Δf_i are not required to be 'smooth'. (Here, by smooth we mean at least of class C^1 .) We will, however, assume that Δf_1 is continuous in x_1 , and that Δf_2 is continuous in x_1, x_2 to guarantee the existence of solutions. Note that uniqueness of solutions is not guaranteed in general.
- (b) f_2 is smooth in x_1, x_2 and $f_2(0, 0) = 0$.

3.2.3. *Controller design.* The development here parallels that given above, and much of it is not repeated.

The first control surface is defined as

$$S_1 = x_1 - x_{1d} \quad (36)$$

We are trying to get x_1 to track x_{1d} . The desired dynamics are $\dot{S}_1 = -K_1 S_1$ with K_1 a positive definite gain matrix. We force the desired dynamics to happen

$$\dot{S}_1 = \dot{x}_1 - \dot{x}_{1d} = x_{2d} + \frac{S_1 \rho_1^2}{2\varepsilon} = -K_1 S_1 \quad (37)$$

The method used to overcome the uncertainty is called ‘nonlinear damping’ (Krstic *et al.* 1995), and ε is a tuning parameter. This can be re-written as

$$x_{2d} = -K_1 S_1 - \frac{S_1 \rho_1^2}{2\varepsilon} + \dot{x}_{1d} \quad (38)$$

In the expression for x_{2d} , the first and third terms provide the desired dynamics, and the second term overcomes the uncertainty. Now that we have an expression for x_{2d} , we use the second differential equation in our system to obtain a control input so that $x_2 \rightarrow x_{2d}$. The second control surface is defined as

$$S_2 = x_2 - x_{2d} \quad (39)$$

The desired dynamics are $\dot{S}_2 = -K_2 S_2$ with K_2 a positive definite gain matrix. We force the desired dynamics $\dot{S}_2 = \dot{x}_2 - \dot{x}_{2d} = \nu_{\text{syn}} + f_2 + \Delta f_2 - \dot{x}_{2d} = -K_2 S_2$, but in doing this we would have to differentiate the expression for \bar{x}_{2d} . Dynamic surface control (DSC) eliminates the need for model differentiation by using first order filters:

$$\tau \dot{\bar{x}}_{2d} + \bar{x}_{2d} = -\frac{S_1 \rho_1^2}{2\varepsilon} - K_1 S_1 + \dot{x}_{1d} \quad (40)$$

with initial condition $\bar{x}_{2d}(0) = x_{2d}(0)$. Then

$$\nu_{\text{syn}} = \dot{\bar{x}}_{2d} - K_2 S_2 - f_2(x_1, x_2) - \frac{S_2 \rho_2^2}{2\varepsilon} \quad (41)$$

3.3. Region of operation

The desired region of operation is chosen as a ball of radius R in \mathcal{R}^n . Consider the following set of (non-linear) algebraic equations

$$\begin{bmatrix} \psi_1 \\ \psi_2 \\ \psi_3 + f_2(\psi_1, \psi_2) \end{bmatrix} = \begin{bmatrix} x_{1d} \\ \dot{x}_{1d} \\ \ddot{x}_{1d} \end{bmatrix} \quad (42)$$

The ψ_i can be solved easily. It can be shown that

$$\|\psi\| = \left\| \begin{bmatrix} \psi_1 \\ \psi_2 \\ \psi_3 \end{bmatrix} \right\| = g(x_d) \quad \text{where } x_d = \begin{bmatrix} x_{1d} \\ \dot{x}_{1d} \\ \ddot{x}_{1d} \end{bmatrix} \quad (43)$$

The function g is smooth (from the smoothness of f_2), $g(0) = 0$ and $g(x_d) \rightarrow \infty$ when $\|x_d\| \rightarrow \infty$. From the smoothness of g , we know that: $\forall R > 0, \exists K_0 > 0$ such that $\|x_d\| < K_0 \Rightarrow g(x_d) = \|\psi\| < R$. The set $\{x_d : \|x_d\| < K_0\}$ is called the set of feasible trajectories.

3.4. Stability of the closed-loop system

Theorem 1 (Boundedness of tracking error using DSC): *Consider any non-Lipschitz non-linear system in the form described earlier. Given any uncertain non-Lipschitz non-linearity with a known C^1 function as its*

upper bound, and given any $p > 0, \varepsilon > 0$, there exists a set of surface gains K_1, K_2 and a filter time constant τ_2 such that the DSC guarantees:

- *Given a desired ball of operation with radius R , there exists a set IC of initial conditions inside the desired ball such that the state of the system is regulated within the ball for all times.*
- *All feasible trajectories can be tracked with a tracking (regulation) error that eventually resides in a ball of radius ε .*

The proof of theorem 1 is given in Girard and Hedrick (2001). It is a variant of a similar proof for a different class of systems, as given in Swaroop *et al.* (2001).

4. Experimental results

A physical demonstration has been conducted to validate the simulation results and show that the DP system performs as predicted. The physical demonstration involves a set of small scale (6 ft long) and economical models to capture the basic hydrodynamic performance of the MOB modules and to capture a representative performance of the thrusters (Spry *et al.* 2000). A scaled module is shown in figure 2.

This scale is small enough to allow three model MOB modules to be floated in a 15m \times 15m indoor model basin at the University of California, Berkeley’s Richmond Field Station (RFS) facility, but large enough to carry the appropriate control computer, actuators and sensors. The modules are kept in alignment and properly positioned with respect to one another exclusively by the use of pivoting thruster units. There are four thrusters per module, and they can each be rotated 360 degrees to produce thrust in any direction in the horizontal plane. Three modules aligned in the tank are shown in figure 3.

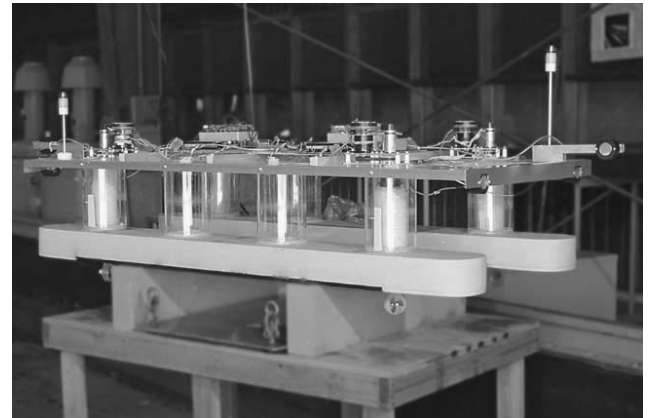


Figure 2. One module of the dynamic positioning experiment.

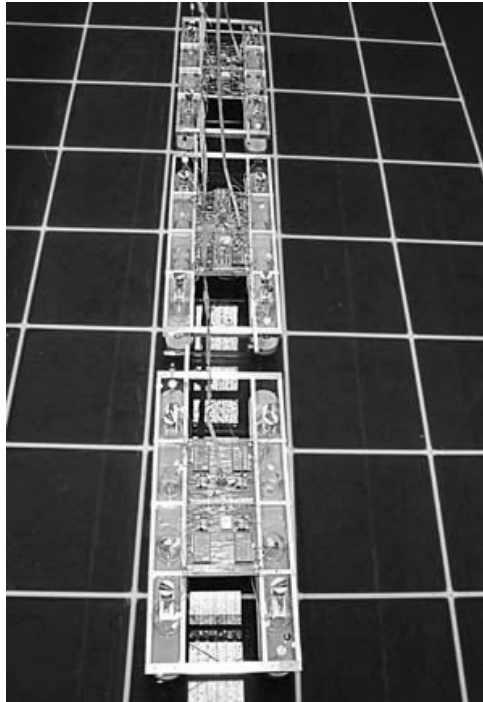


Figure 3. Coordinated dynamic positioning, from above.

4.1. Dynamic positioning system for one module using DSC

Dynamic positioning is a complex control problem and we have partitioned it into several layers, including the DP law itself, the thruster allocation logic (TAL), and thruster control. The DP law takes as input a desired position or trajectory to track, and produces a desired force and moment vector to be applied on the module. The TAL uses this desired force and moment vector to produce thrust and slew commands for the individual thrusters, while taking into account the physical capabilities of the thrusters and optimizing fuel consumption (Webster *et al.* 1999). The low-level thrust control uses look-up tables to ensure that the behaviour of the scaled thrusters is representative of what a full-scale thruster could achieve on a full-sized MOB module. In this section we concern ourselves with the behaviour of the complete system. The interplay of the different layers is described in great detail in Girard *et al.* (2000). As the parameters for the experiment are fairly well known, we have implemented the robust version of the DSC control law as presented above, consisting of equations (5), (7), (9), (11) and (16) for the single module case, and of equations (17–19, 7, 9, 11 and 16) for the coordinated case.

Figure 4 presents data for a dynamic positioning (station-keeping) test run in the Berkeley tank. Only one module was used for this test. The surge, sway and yaw motions of the module are shown for a test

period of 450 s. The performance is within ± 2 cm in surge and sway, and within ± 1 degree in yaw; this is on the order of the accuracy of the sensing system.

4.2. Coordinated, multi-module dynamic positioning system

We now consider the performance of the coordinated DP system. There is no convenient way to control initial conditions and hold the modules in the water prior to starting the control system. For safety reasons, at start-up, each module defaults to individual (non-coordinated) DP. Figure 5 shows the behaviour of module 1 during a coordinated DP run. The coordinated controller was started at $t = 42$ s. Once the controller is started we observe exponential behaviour towards the desired position.

For the run presented in figure 5, the gains placed on the relative position of the modules were identical to the gains placed on the absolute position of the modules in the tank.

4.3. Hybrid system specification of docking communication protocol

Manoeuvre switching is specified using hybrid system formalisms, which interface high-level supervision (discrete) with the continuous dynamic surface control laws for each platform. To do this we use basic manoeuvres. A trajectory/reference generator, pre-conditions (that determine the validity of the initial conditions for the manoeuvre), invariants (that specify conditions under which the manoeuvre is valid) and termination conditions form a basic manoeuvre. All these conditions can be enabled or disabled. Only one manoeuvre is active at any given time.

The controllers in the manoeuvre coordination layer (off, dynamic positioning, coordinated DP, assemble, separate, rotate into the wind) send desired acceleration set points to the dynamic surface controller.

Each controller is formed of a control law, and a ‘protocol’ that is used to coordinate manoeuvres. The current design uses protocols in the form of finite state machines to organize the manoeuvres in a systematic way. They receive commands from the supervisory controller and aggregated information from the individual platforms, then use this information to decide on a control policy and issue commands to the DP controllers.

As an example, the protocol for the ‘assemble a MOB’ controller is given here. It is formed of two state machines, one for each platform involved. For simplicity, we call the platforms ‘stationary’ and ‘moving’ throughout the following description. The state machine containing the logic for the stationary platform is presented in figure 6. The state machine containing the logic for the moving platform is presented in figure 7.

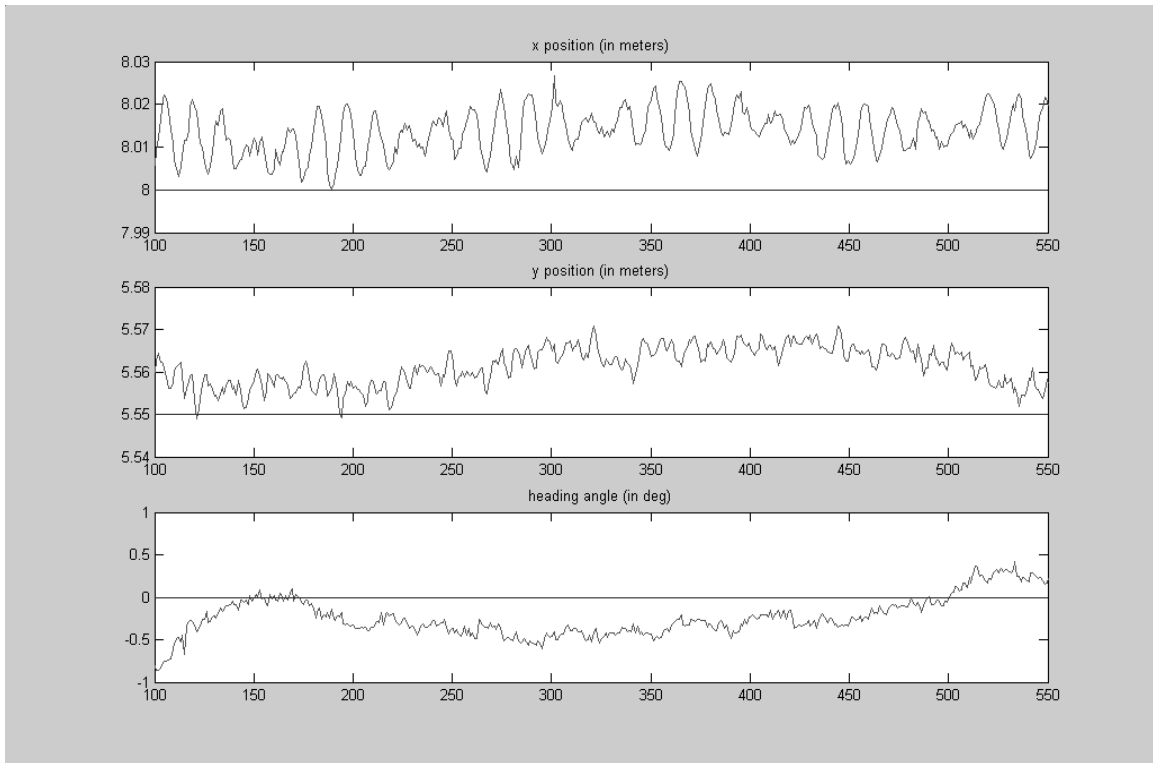


Figure 4. Dynamic positioning of one module about (8 m, 5.55 m, 0 degrees). Surge, sway and yaw motions vs. time.

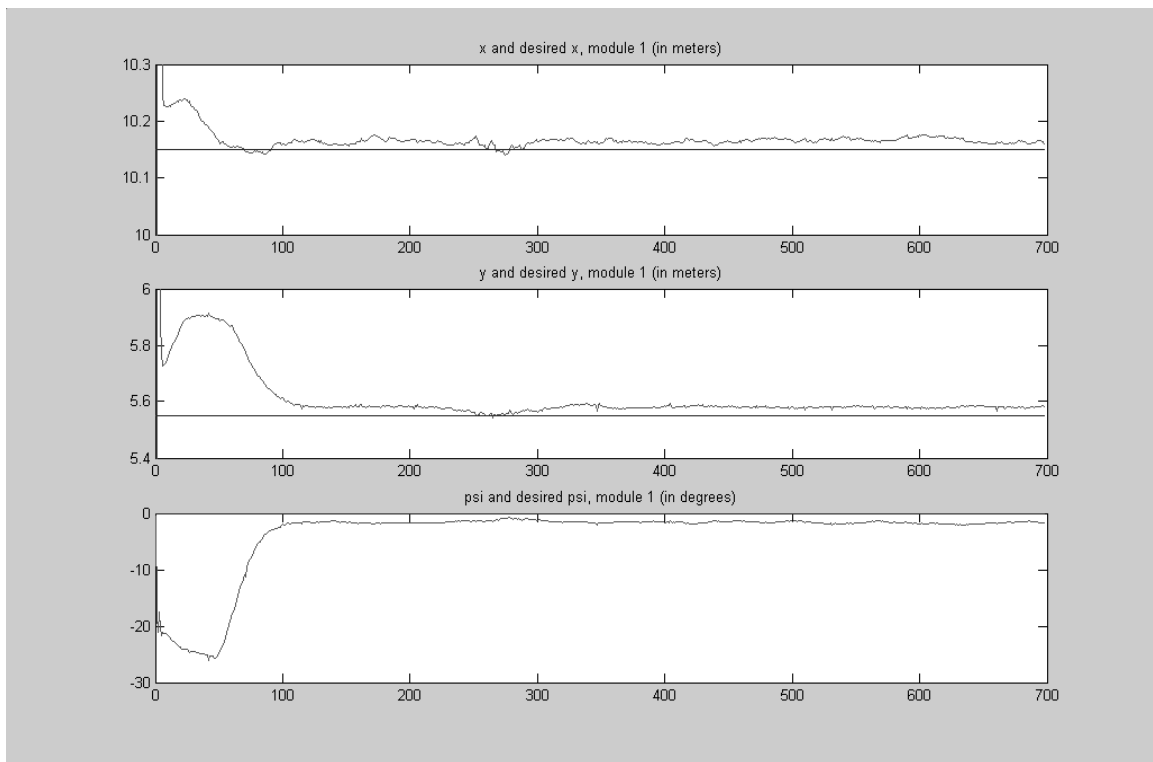


Figure 5. Module one—coordinated DP run about (10.15 m, 5.55 m, 0 degrees). Surge, sway and yaw motions of the first module in the assembly vs. time.

The stationary platform gets a request asking it whether it is available for assembly; if not a time out occurs and the manoeuvre is aborted, and if yes the stationary platform ‘blocks’ itself so that no other platform may join while the manoeuvre is taking place.

When the manoeuvre is complete, the stationary platform starts coordinated dynamic positioning operations.

The moving platform asks the stationary platform for permission to join. If it is not granted, the moving platform goes back to independent operation; otherwise it starts its approach towards the stationary platform. A trajectory is computed for the ‘join’ manoeuvre. This trajectory is communicated to the lower level controller that regulates the moving platform.

When the platforms have joined, coordinated dynamic positioning is activated; the moving platform enters coordinated operation. The system can be set so, at this point, both platforms make themselves available to join.

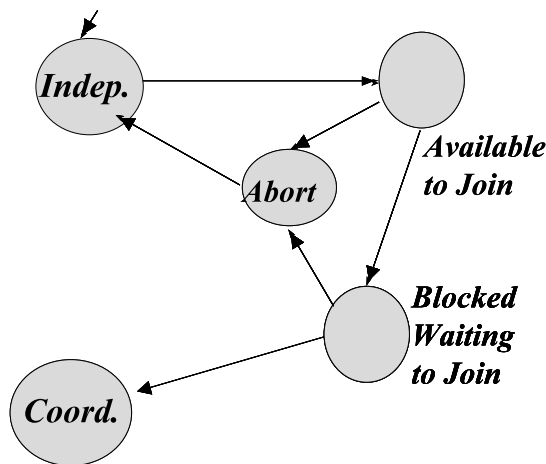


Figure 6. State machine for stationary platform.

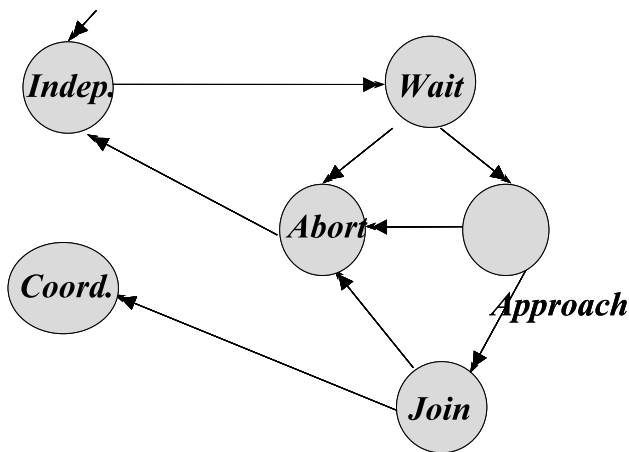


Figure 7. State machine for moving platform.

The docking manoeuvre is the most difficult manoeuvre in the whole set of manoeuvres that MOB modules may be called upon to perform, because of the inherent risk of collision between adjacent modules. Also, in the eventuality that someone designed a feasible connector for an assembly such as a MOB, the connector would probably require momentum to engage; that is the modules would have to dock with a non-zero relative velocity, so that the connector would click in. This would further increase the risk of collision.

A (connector-less) docking manoeuvre has been implemented on the scaled modules and is done in two steps. First, all the modules align at a respectable distance from each other. Then, the ‘end’ modules come in slowly to a specified distance from the centre module.

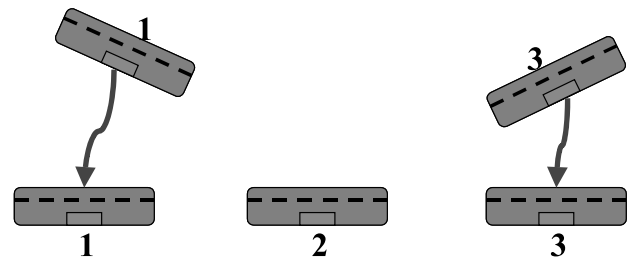
Figure 8 shows the two-step organization of the docking procedure.

Figure 9 shows the control in the surge direction, for each module, during the second step of the docking manoeuvre. The modules lag a bit behind the reference trajectory due to high damping in the tank and there is no overshoot. The damping in the tank appears to be higher than predicted by simulations and one possible explanation for this may be the presence of significant un-modelled hydrodynamic interactions between the modules and the bottom of the tank. The modules have gone through the series of ‘handshakes’ and communication protocols as described above.

5. Concluding remarks

In this work, we have discussed the design and implementation of a regulation and tracking controller for a MOB. A MOB is formed of several modules, which must remain aligned at sea to form

STEP ONE



STEP TWO

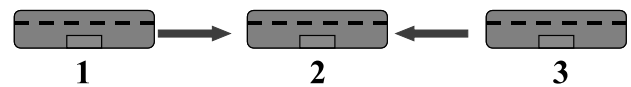


Figure 8. Docking procedure for the scaled MOB experiment, step 2.

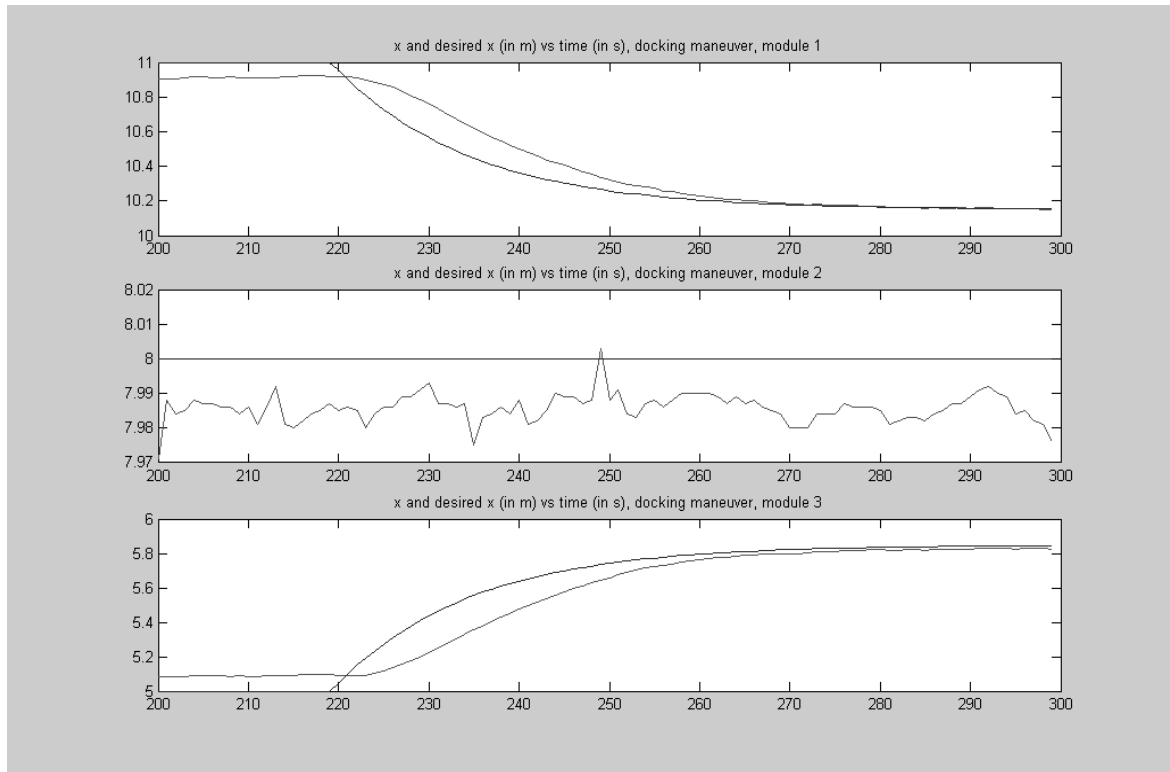


Figure 9. Docking procedure for the MOB experiment, step 2.

a runway and provide support for military operations where land bases are not available or adequate. The MOB modules must perform long-term station keeping at sea in the presence of wind, waves and currents; this is referred to as dynamic positioning. As the disturbances are likely to come from all directions, the modules are equipped with four pivoting thrusters so as to be able to produce forces and moments in surge, sway and yaw. The most important factor to be able to land planes on the MOB is the alignment of the runway. The relative position of the different modules must be very tight, but the whole assembly is allowed to drift within reason.

There are several possible choices for the DP controller, and in this work we have selected one based on DSC. The setpoints come from higher layers of control or human operators. The DP controller decides on a desired force and moment system for each module. The dynamic surface controller uses low-pass filters to avoid model differentiation, thereby circumventing the classical ‘explosion of terms’ problem. Arbitrarily tight semi-global regulation is guaranteed.

The authors and members of the California PATH program did much full-scale simulation work during the MOB project. The interested reader is referred to Girard *et al.* (2001).

The controller performance was verified experimentally using scaled modules. The scaled modules were built at Berkeley to validate the feasibility of multi-module coordinated dynamic positioning. The sensing and actuating systems for the modules are briefly discussed, as they are instrumental to the DP performance. The robust version of the control law was chosen, as the hydrodynamic characteristics of the scaled modules are fairly well known, and as the scaled modules are not subject to loading variations during operations. Experimental results for the controller were presented, and the tracking performance is shown to be on the order of ± 2 cm in surge and sway, and $\pm 1^\circ$ in yaw. This is comparable to the performance of the sensing and state estimation systems. Results for coordinated DP control are presented as well. Video of the scaled modules in the tank is available from the authors’ web page: <http://path.berkeley.edu/~anouck/mob2.html>

Acknowledgements

The authors would like to thank João Borges de Sousa and the experimental group at California PATH for their help during the MOB project, and the reviewers for their careful lecture of the manuscript. Pictures are courtesy of Gerald Stone from PATH publications.

References

- FOSSEN, T. I., 1994, *Guidance and Control of Ocean Vehicles* (Chichester: Wiley).
- GIRARD, A. R., 1999, Nonlinear dynamic positioning of ships and/or offshore structures. ME237 final report, Dept. of Mechanical Engineering, University of California at Berkeley.
- GIRARD, A. R., BORGES DE SOUSA, J., WEBSTER, W. C., and HEDRICK, J. K., 2001, Simulation environment design and implementation: an application to the mobile offshore base. *Proceedings of the 20th International Conference on Offshore Mechanics and Artic Engineering, OMAE*, Rio de Janeiro, Brazil, pp. 2061–2070.
- GIRARD, A. R., and HEDRICK, J. K., 2001, Dynamic positioning of ships using nonlinear dynamic surface control. *Proceedings of the Fifth IFAC Symposium on Nonlinear Control Systems*, Saint-Petersburg, Russia, 4–6 July, pp. 1134–1140.
- GIRARD, A. R., HEDRICK, J. K., and BORGES DE SOUSA, J., 2000, A hierarchical control architecture for mobile offshore bases. *Marine Structures Journal*, **13**, 459–476.
- HEDRICK, J. K., GIRARD, A. R., and KABU, B., 1999, A coordinated DP control methodology for the mobile offshore base. *Proceedings of the ISOPE*, Brest, France, pp. 70–75.
- KHALIL, H. K., 2001, *Nonlinear Systems*, 3rd edn (Upper Saddle River, NJ: Prentice Hall).
- KRSTICK, M., KANELAKOPOULOS, I., and KOKOTOVIC, P., 1995, *Nonlinear and Adaptive Control Design* (New York: Wiley Interscience).
- NEWMAN, J., 1977, *Marine Hydrodynamics* (Cambridge, MA: MIT Press).
- SLOTINE, J. J. E., and LI, W., 1991, *Applied Nonlinear Control* (Englewood Cliffs, NJ: Prentice Hall).
- SPRY, S. C., EMPEY, D. M., and WEBSTER, W. C., 2000, Design and characterization of a small-scale azimuthing thruster for a mobile offshore base module. *Marine Structures Journal*, **14**, 215–229.
- SWAROOP, D., and HEDRICK, J. K., 1996, String stability of interconnected systems. *IEEE Transactions on Automatic Control*, **41**, 349–357.
- SWAROOP, D., HEDRICK, J. K., YIP, P. P., and GERDES, J. C., 1997, Dynamic surface control of nonlinear systems. *Proceedings of the American Control Conference*, New Mexico, USA, Vol. 5, pp. 3028–3034.
- SWAROOP, D., HEDRICK, J. K., YIP, P. P., and GERDES, J. C., 2001, Dynamic surface control for a class of nonlinear systems. *IEEE Transactions on Automatic Control*, **45**, 1893–1899.
- UTKIN, V. I., 1992, *Sliding Modes in Control Optimization* (New York: Springer-Verlag).
- UTKIN, V. I., 1977, Variable structure systems with sliding modes. *IEEE Transactions on Automatic Control*, **AC-22**, 212–222.
- UTKIN, V., GULDNER, J., and SHI, J., 1999, *Sliding Mode Control of Electromechanical Systems* (London: Taylor & Francis).
- WEBSTER, W. C., and SOUSA, J. B., 1999, Optimum allocation for multiple thrusters. *Proceedings of the ISOPE*, Brest, France, pp. 83–89.
- WON, M., and HEDRICK, J. K., 1996, Multiple surface sliding control of a class of uncertain nonlinear systems. *International Journal of Control*, **64**, 693–706.